ELSEVIER

Open-circuit test of a PZT vibrator and its applications

Kuo-Tsi Chang [a,b,*], Minsun Ouyang [a]

[a] *Department of Engineering and System Science, National Tsing-Hua University, 101, Section 2 Kuang Fu Road, Hsinchu 30043, Taiwan, ROC*
[b] *Department of Electrical Engineering, National Lien-Ho College of Technology, 1 Lien-Kung Road, Kungjing Li, Miaoli 36012, Taiwan, ROC*

Abstract

This study investigates a terminal transient response of a Langevin-type PZT vibrator theoretically and experimentally to quantify an electrical shock and refine an equivalent circuit of the vibrator. The shock is induced immediately after an AC sinusoidal voltage of the vibrator is switched off. Then, the transient response involves a DC part and an AC part, which approach zero at the DC and AC times, respectively, and the vibrator is placed on a sponge in air. To do so, we should propose an open-circuit test to find the AC and DC times in addition to the maximum amplitude of the transient response. Thus the DC times exceeds the AC time, and the AC and DC times are used to estimate the resistances in the equivalent circuit presenting the real mechanical and dielectric losses, respectively. Therefore, the resistances in the equivalent circuit are sensitive to the vibration amplitude, but the inductance and capacitances are not. Furthermore, the maximum amplitude is required to cause the shock, and depends on the frequency of the source and the open-circuited time, and is about 65 times the amplitude of the source.
© 2002 Elsevier Science B.V. All rights reserved.

1. Introduction

Electric shocks with high-voltage transient responses at the terminals of vibrators under high-power excitation are induced after the related drives are switched off. These shocks have not yet been investigated. An "a R_s–L_s–C_s branch parallels parameters of R_p and C_p" impedance model has not been built into an impedance analyzer (HP4194A) to measure resistance as the dielectric loss of vibrators. For a resistance equivalent to the real mechanical loss, the high-power constant differs from the low-power constant measured by the analyzer.

A differential circuit has been proposed to measure separately the mechanical loss and the dielectric loss by detecting the motional admittance under high-power excitation [1]. Moreover, terminal voltage and current have been used to determine dielectric loss just after switching on the high-power drive, and the force factor and the attenuation constant have been used to estimate

the high-power equivalent resistance [2]. This factor resembles the ratio of the amplitude of the motional current to the amplitude of the vibration velocity and was used to estimate short-circuit transient response of a terminal current after the drive was switched off. These methods constitute very complicated ways to calculate the equivalent resistance and cannot analyze electric shocks for purely AC transient response.

Accordingly, an open-circuit test is proposed to elucidate complete terminal transient responses of vibrators under high-power excitation for quantifying electric shocks and estimating equivalent resistive constants. The test can reveal how to reduce the highest voltage of the shock and simply refine the high-power equivalent circuit.

2. Equivalent circuit of the vibrator

An equivalent circuit of a PZT vibrator with initial conditions, illustrated in Fig. 1(a), is employed to derive a terminal voltage with an open-circuit transient response. Another equivalent circuit connected to an AC voltage $v_s(t) = V_s \sin \omega_s t$, shown in Fig. 1(b), is applied

---
* Corresponding author. Address: Department of Electrical Engineering, National Lien-Ho College of Technology, 1 Lien-Kung Road, Kungjing Li, Miaoli 36012, Taiwan, ROC.
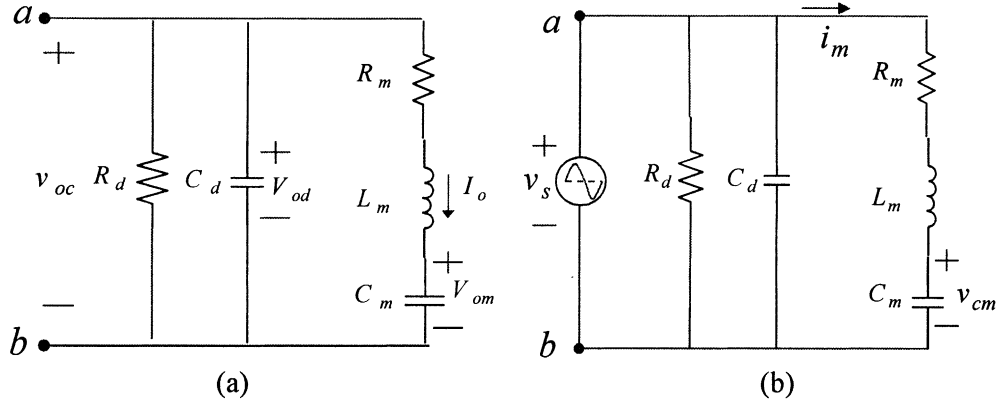
Fig. 1. Equivalent circuits of a PZT vibrator with: (a) initial conditions and (b) an AC voltage.

Table 1
Description of the parameters in Fig. 1

Parameters	Descriptions
R_d	Equivalent resistance indicating real dielectric loss
R_m	Equivalent resistance indicating real mechanical loss
C_d	Damped capacitance of the piezoelectric ceramic
L_m	Equivalent inductance indicating equivalent mass
C_m	Equivalent capacitance indicating equivalent stiffness

to derive steady responses of v_{cm} and i_m. Table 1 describes the parameters in Fig. 1. The mechanical resonant frequencies of vibrators are given calculated by $f_m = 1/(2\pi(L_mC_m)^{1/2})$ and $f_{ar} = 1/(2\pi(L_mC_{md})^{1/2})$ where $C_{md} = C_mC_d/(C_m + C_d)$. Here, f_m and f_{ar} are the resonant frequency and the anti-resonant frequency, respectively. Then the mechanical quality factor, Q_m, is determined using, $Q_m = \omega_mL_m/R_m$ where $\omega_m = 2\pi f_m$.

3. Analysis of transient and steady responses

From Eq. (A.2) in Appendix A, the diagrams of the voltage v_{oc} are indicated in Fig. 2, and $f_{oc} = \beta/2\pi \cong f_{ar}$

where f_{oc} represents the oscillated frequency of v_{oc}. The maximum amplitudes of DC and AC responses of v_{oc} are related to the initial conditions, V_{od}, V_{om} and I_0. The DC response $be^{-\alpha_{dc}t}$ almost vanishes after DC steady-state time t_{dc} ($= 5R_dC_d$) is reached, and the AC response $fe^{-\alpha_{ac}t}\cos(\beta t - \varphi)$ nearly vanishes after AC steady-state time t_{ac} ($= 10L_m/R_m$) is reached. Consequently, R_d and R_m can be calculated since t_{dc}, t_{ac}, C_d and L_m are known.

Next, the initial conditions are calculated by the following steady-state responses: let $v_s(t) = V_s \sin \omega_m t$ where h denotes the high-power excitation at the first resonant frequency, then $v_{cm}(t) = Q_mV_s\sin(\omega_m t - \pi/2)$, $i_m(t) = I_{mh}\sin \omega_m t$ and $I_{mh} = V_s/R_m$. Table 2 lists various initial conditions and their corresponding amplitudes of b and f in Eq. (A.2). The high-power highest voltage, $V_{oc,max}^h$, is determined by (Fig. 3)

$$V_{oc,max}^h \cong |b| + f \cong (2Q_mC_m/C_d)V_s. \tag{1}$$

Moreover, let $v_s(t) = V_s \sin \omega t$ where 1 represents the low-power excitation near and above the first resonant frequency, then $v_{cm}(t) = G_{cm}V_s\sin(\omega t - \varphi_{im} - \pi/2)$, $i_m(t) = I_{ml}\sin(\omega t - \varphi_{im})$, $G_{cm} = 1/(\omega C_m|Z(\omega)|)$,
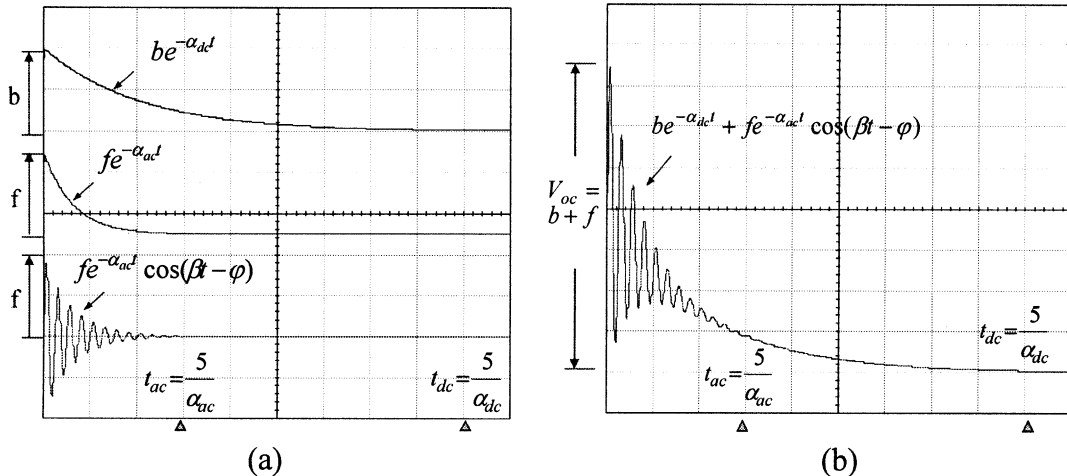

Fig. 2. Schematic waveforms of the transient response: (a) the DC and AC parts individually and (b) a complete transient response.

Table 2
Maximum amplitudes and drive conditions

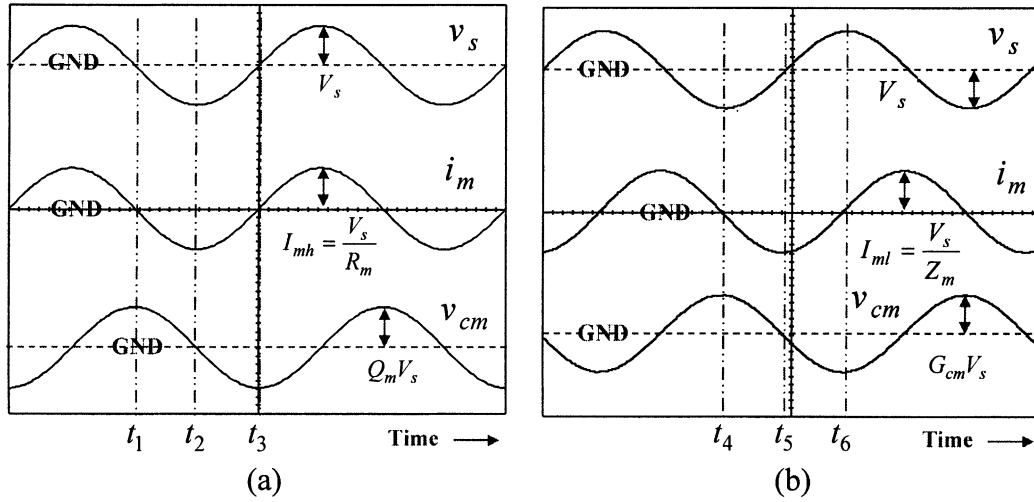| AC voltages at frequencies	At open-circuited times in Fig. 3	Drive conditions			Maximum amplitudes, $V_{oc}^+ = b + f(b > 0)$ or $V_{oc}^- = b + f(b < 0)$
		V_{od}	V_{om}	I_0	
$f_s = f_m$	t_1	0	$Q_m V_s$	0	$V_{och}^+ = 2(C_m Q_m / C_d) V_s$
	t_2	$-V_s$	0	$-I_{mh}$	$V_{och}^0 = -V_s + I_{mh} / \beta C_d$
	t_3	0	$-Q_m V_s$	0	$V_{och}^- = (-1) \times V_{och}^+$
$f_s > f_m$	t_4	$-V_s$	$G_{cm} V_s$	0	$V_{ocl}^+ = 2(C_m G_{cm} / C_d - 1) V_s$
	t_5	0	0	$-I_{ml}$	$V_{ocl}^0 = I_{ml} / \beta C_d$
	t_6	V_s	$-G_{cm} V_s$	0	$V_{ocl}^- = (-1) \times V_{och}^+$

Fig. 3. Schematic waveforms of steady-state responses: (a) for resonance and (b) for above resonance.

$I_{ml} = V_s / |Z(\omega)|$, $\varphi_{im} = \arctan(1/(\omega C_m R_m))$ and $Z(\omega) = R_m + j(\omega L_m - 1/(\omega C_m))$. The low-power highest voltage, $V_{oc,max}^l$, is calculated by

$$V_{oc,max}^l \cong |b| + f \cong (2G_{cm} C_m / C_d - 1) V_s. \tag{2}$$

4. Design of drive system

The drive system of the open-circuit test includes an inverter circuit, signal circuits and a switch system, as illustrated in Fig. 4. From Fig. 4(a) [3], the inverter circuit consists of a DC/DC buck converter, a full-bridge switching chopper, a filter and an equivalent circuit of the vibrator, and thus generates AC sinusoidal voltages of the vibrator. When S_1 and S_4 are ON and S_2 and S_3 are OFF, the amplitude of v_{sqr} is V_{in}. When S_1 and S_4 are OFF and S_2 and S_3 are ON, the amplitude of v_{sqr} is $-V_{in}$. Meanwhile, the frequency of v_{sqr} is identical to that of rectangular gate-to-source voltages, v_{gs1-4}, with an on-duty cycle of 50%. The switches, S_{1-4}, are implemented by MOSFET devices (IRF840).

From Fig. 4(b), pulse-width modulation and voltage-controlled oscillator circuits are used to control the voltage and frequency of AC sources, respectively, and implemented by UC3524 and LM566, respectively. Next, the switch system shown in Fig. 4(c) performs the switch SW displayed in Fig. 4(a), and comprises a function generator (Agilent, 33120A), a MOSFET device (IRF840) and a relay (DC 12 V, JZC-6F, 4098). Then, the MOSFET S_{sw} is controlled by a rectangular gate-to-source voltage, v_{sw} (1 Hz, 0 V/12 V) that is obtained from the function generator. In Fig. 4(d), a schematic waveform of v_{oc} is obtained after time t_{dsw} at the turned-on time of the MOSFET S_{sw}.

5. Verification results

5.1. Measured results of the transient response and AC voltage

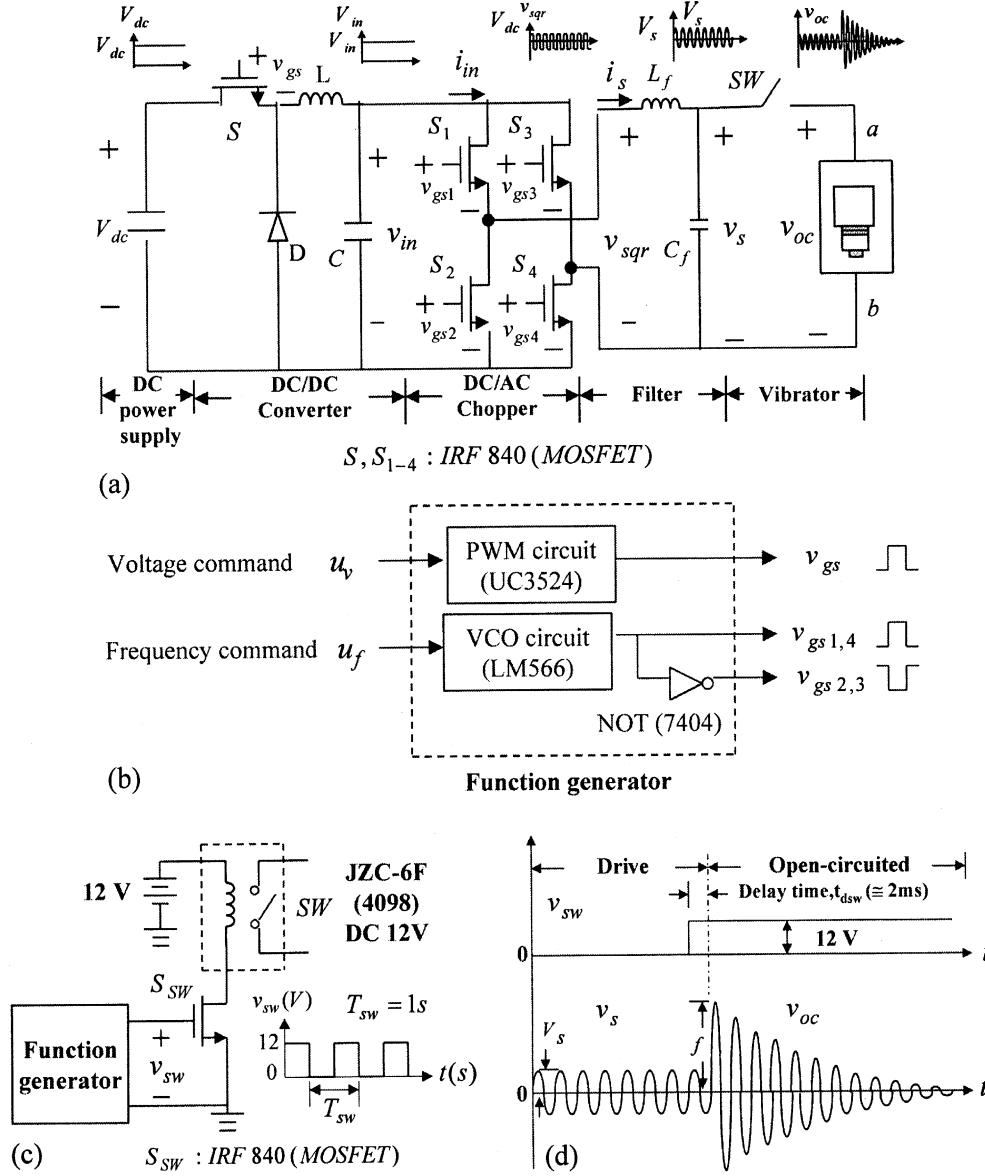A Langevin-type PZT vibrator (BLT-45282H) (diameter, 45 mm; length, 79.5 mm; mass, 411 g)

Fig. 4. Block diagrams of drive system: (a) an inverter circuit, (b) function generators, (c) a switch system, and (d) a schematic waveform of the transient response obtained after time t_{dsw} at the turned-on time of the MOSFET S_{sw}.

manufactured by Increase-More Industrial Corp. in Taiwan is used in the test. The parameters of the vibrator are then measured using an impedance analyzer HP4194A: $R_m^A = 174.6\ \Omega$, $L_m = 122.1$ mH, $C_m = 0.243$ nF, $C_d = 3.79$ nF, $f_m = 29.22$ kHz and $f_{ar} = 30.13$ kHz. Moreover, the waveforms of v_{oc} in Figs. 5, 6, 7(a, b) and (c, d) are induced by sinusoidal voltages v_{s1} (10 V/29.22 kHz), v_{s2} (10 V/29.41 kHz), v_{s3} (30 V/29.22 kHz) and v_{s4} (30 V/29.41 kHz), respectively. Meanwhile, the voltages are obtained using the parameters, L_f ($\cong 143$ μH) and C_f ($\cong 0.1$ μF) in Fig. 4(a), and the waveforms are measured using a probe with a ratio of 1/100 and an oscilloscope (YOKOGAWA, DL1520). From Fig. 5, the observed waveforms are obtained after about 2 ms at the turned-

on time of the MOSFET S_{sw} in Fig. 4(c) due to the delay of the switch system. Additionally, the waveforms of the DC part of v_{oc} are measured by the smooth-and-filter function of the oscilloscope, and thus $b \cong 280$ V obtained from Fig. 5(a) or (b) and $b \cong 320$ V measured from Fig. 5(c) or (d).

5.2. The measured times and the estimated results

According to Table 3, the DC time (about 180 ms) exceeds the AC time (around 46 or 48 ms), and thus $R_m^1 \cong R_m^3 \cong 26.5\ \Omega$ estimated using $t_{ac}^1 \cong t_{ac}^3 \cong 46$ ms; $R_m^2 \cong R_m^4 \cong 25.4\ \Omega$ obtained using $t_{ac}^1 \cong t_{ac}^3 \cong 48$ ms, where the superscripts 1–4 represent the results
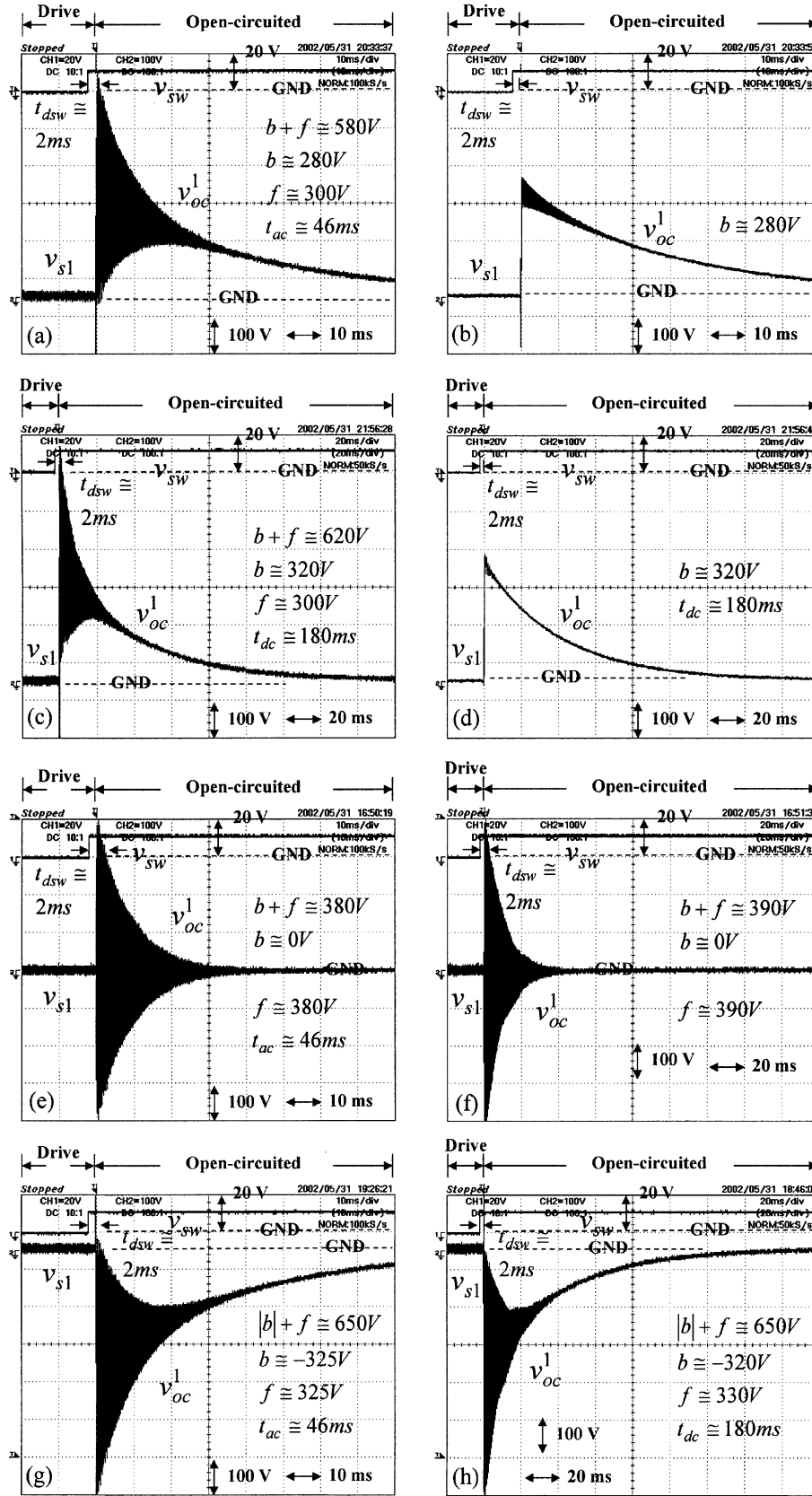
Fig. 5. Observed waveforms induced after the source v_{s1} is switched off at various times: (a)–(d) at time t_1, (e) and (f) at time t_2, and (g) and (h) at time t_3. The waveforms in (b) and (d) are measured using the smooth-and-filter function of the oscilloscope. The times, involving t_1, t_2 and t_3, are displayed in Fig. 3(a).
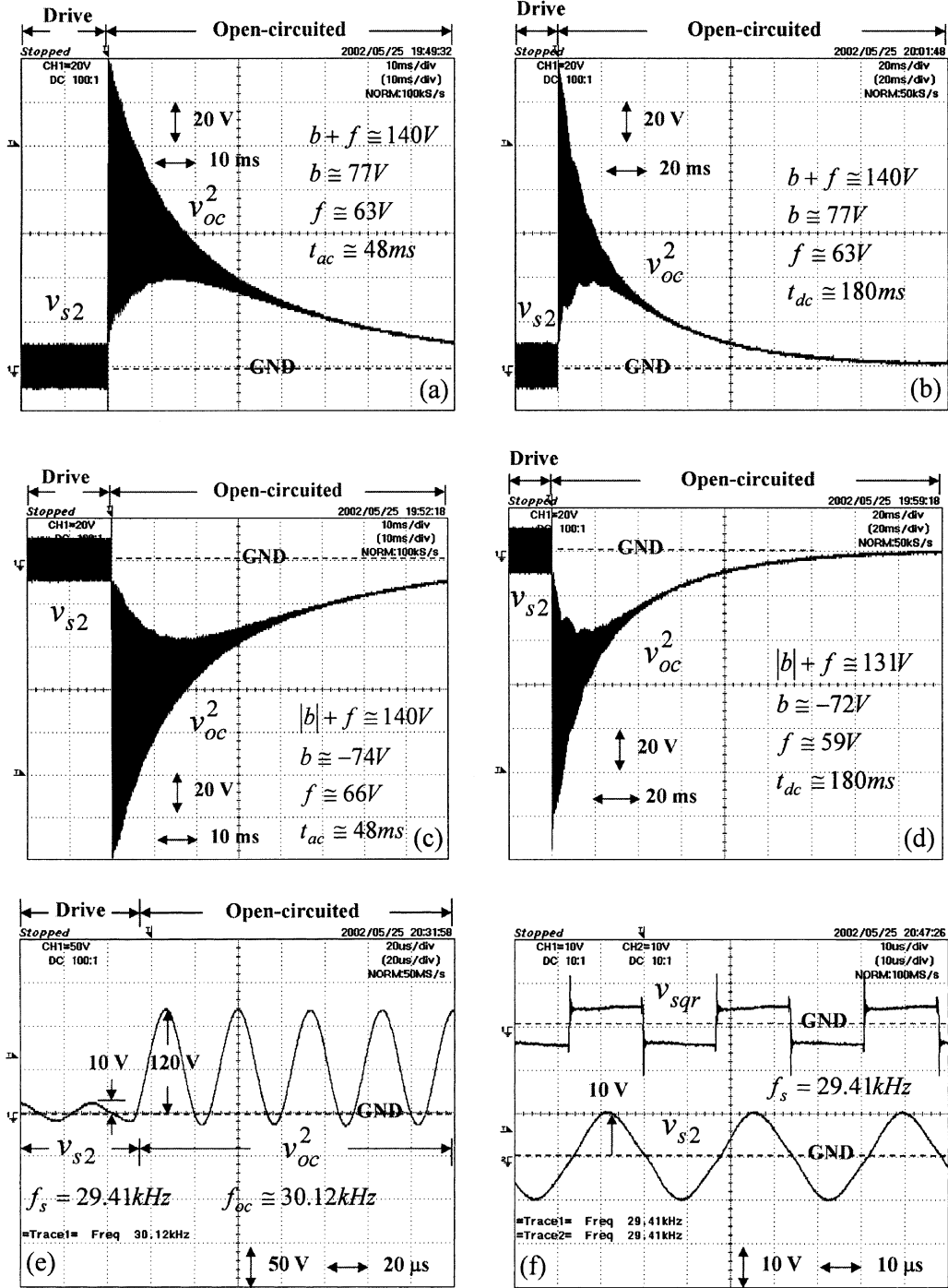
Fig. 6. Observed waveforms induced after the source v_{s2} is switched off at various times: (a) and (b) at time t_4, (c) and (d) at time t_6, and (e) near time t_4. The waveforms in (f) indicates the sources of v_{sqr} and v_{s2}. Both t_4 and t_6 are displayed in Fig. 3(b).

concerning the voltages v_{s1-4}, respectively. Then, $R_d \cong$ 190 MΩ and $R_{d1} \cong 9.5$ MΩ estimated by $R_d = R_{d1}R_{scope}/(R_{scope} - R_{d1})$ and $R_{d1} \cong t_{dc}/5(C_d + C_{scope})$, respectively, and $t_{dc} \cong 180$ ms obtained from Table 3. Here, R_{scope} and C_{scope} represent the impedance of the probe and oscilloscope, as shown in Fig. 8(b); $R_{scope} \cong 10$ MΩ and $C_{scope} \cong 3.73$ pF measured by the impedance analyzer. Therefore, $R_{scope}(\ll R_d)$ influences the DC time and the

estimated result of R_d at the open state, but $C_{scope}(\ll C_d)$ does not.

5.3. The maximum amplitudes and drive conditions

From Table 4, the magnitude of $V_{oc,max}^1$ ($\cong 650$ V) exceeds that of $V_{oc,max}^2$ ($\cong 140$ V), and the magnitude of $A_{oc,max}^1$ ($\cong 65$) exceeds that of $A_{oc,max}^2$ ($\cong 14$); the mag-
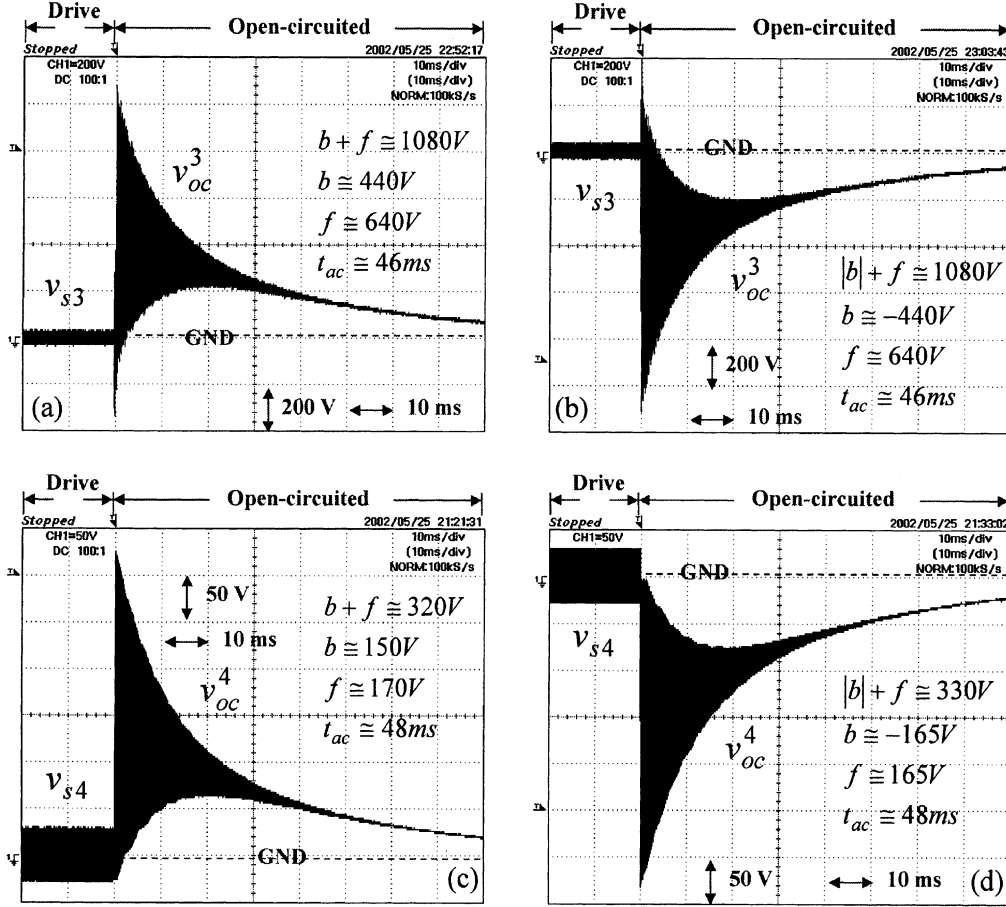
Fig. 7. Observed waveforms induced after the sources v_{s3} and v_{s4} are switched off at various times: (a) and (b) at time t_1, and (c) and (d) at time t_3.

Table 3
Magnitude of the measured times and estimated results

From figures	The measured times		Estimated results			
	t_{ac} (ms)	t_{dc} (ms)	R_m (Ω)	R_{dl} (MΩ)	R_d (MΩ)	Q_m
5 and 7(a, b)	46	180	26.5	9.5	190	844
6 and 7(c, d)	48	180	25.4	9.5	190	881

nitude of $V_{oc,max}^3$ ($\cong 1080$ V) exceeds that of $V_{oc,max}^4$ ($\cong 330$ V), and the magnitude of $A_{oc,max}^3$ ($\cong 36$) exceeds that of $A_{oc,max}^4$ ($\cong 11$). Here, $V_{oc,max}^i = \max\{V_{oc,max}^{i(+)}, |V_{oc,max}^{i(-)}|\}$ and $A_{oc,max}^i = V_{oc,max}^i/V_{si}$ for $i = 1$–4, where $V_{oc,max}^{(+)}(= b + f, b > 0, f > 0)$ and $V_{oc,max}^{(-)}(= -|b| - f, b < 0, f > 0)$ represent the positive and negative maximum amplitude of v_{oc}, respectively. For the resonance operations, $V_{oc,max}^{1(+)}$ and $V_{oc,max}^{1(-)}$ are obtained at the open-circuited time t_1 and t_3 in Fig. 3(a), respectively, and $V_{oc,max}^{3(+)}$ and $V_{oc,max}^{3(-)}$ are also. For the above resonance operations, $V_{oc,max}^{2(+)}$ and $V_{oc,max}^{2(-)}$ are obtained at the open-circuited time t_4 and t_6 in Fig. 3(b), respectively, and $V_{oc,max}^{4(+)}$ and $V_{oc,max}^{4(-)}$ are also.

Regarding the sign of b, $b > 0$, obtained at the open-circuited time in the interval between t_1 and t_2 in Fig. 3(a), as shown in Figs. 5(a)–(d) and 7(a), or between t_4 and t_5 in Fig. 3(b), as displayed in Figs. 6(a, b) and 7(c). Then, $b < 0$, obtained at the open-circuited time in the interval between t_2 and t_3, as shown in Figs. 5(g, h) and 7(b), or between t_5 and t_6, as displayed in Figs. 6(c, d) and 7(d). Moreover, $b \cong 0$, obtained at the open-circuited time t_2 or t_5, as shown in Fig. 5(e,f).

6. Discussion

The following observations prove that L_m, C_m and C_d are insensitive to the vibration amplitude of the vibrator. (1) The oscillated frequency (about 30.12 kHz in Fig. 6(e)) almost equals the anti-resonant frequency (around 30.12 kHz). (2) The maximum voltage of the transient response and the maximum current of the vibrator are obtained by the source at the resonant frequency (about 29.22 kHz). (3) The magnitude of R_m^A ($\cong 174.6$ Ω) exceeds that of R_m^1 ($\cong R_m^3 \cong 26.5$ Ω) or R_m^2 ($\cong R_m^4 \cong 25.4$ Ω), according to Table 3. (4) From
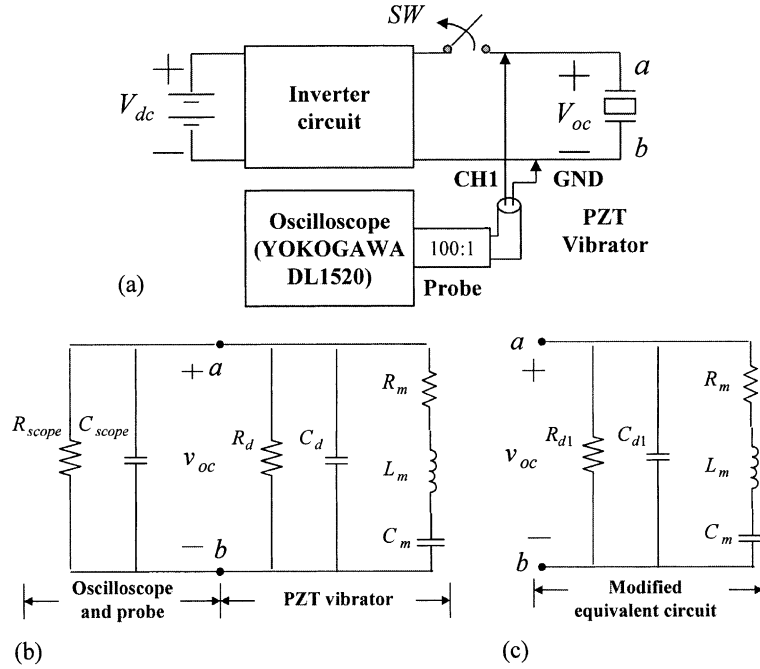
Fig. 8. Modification of equivalent circuit: (a) a diagram of the measuring system, (b) equivalent circuits of the vibrator and the measuring system, and (c) a modified equivalent circuit.

Table 4
Magnitude of the maximum amplitudes

Items	From figures	AC voltages		At open-circuited time t_{1-6} in Fig. 3	Maximum amplitudes	
		Amplitude V_s (V)	Frequency f_s (kHz)		Magnitude $V_{oc,max}$ (V)	Sign (+ or −)
$V_{oc,max}^{1(+)}$	5(c)	10	29.22	t_1	620	+
$V_{oc,max}^{1(-)}$	5(g)			t_3	650	−
$V_{oc,max}^{2(+)}$	6(a)		29.41	t_4	140	+
$V_{oc,max}^{2(-)}$	6(c)			t_6	140	−
$V_{oc,max}^{3(+)}$	7(a)	30	29.22	t_1	1080	+
$V_{oc,max}^{3(-)}$	7(b)			t_3	1080	−
$V_{oc,max}^{4(+)}$	7(c)		29.41	t_4	320	+
$V_{oc,max}^{4(-)}$	7(d)			t_6	330	−

Table 5
Comparison of open-circuit test and impedance analyzer methods

Methods	Magnitude of R_m (Ω)	AC times t_{ac} (ms)	Maximum amplitudes		AC voltages	
			V_{oc}, max (V)	$A_{oc,max}$	Amplitude V_s (V)	Frequency f_s (kHz)
Open-circuit test	26.5 (15.2%)	46	650	65	10	29.22
			1080	36	30	
Impedance analyzer	174.6 (100%)	7.0	93	9.3	10	29.22
			164	5.5	30	

Table 5, the magnitude of $V_{oc,max}^{1}$ ($\cong 650$ V) exceeds largely that of $V_{oc,max}^{1A}$ ($\cong 93$ V) and the magnitude of $V_{oc,max}^{3}$ ($\cong 1080$ V) exceeds greatly that of $V_{oc,max}^{3A}$ ($\cong 164$ V). Here, $V_{oc,max}^{1A}$ and $V_{oc,max}^{3A}$ are calculated using $R_m^A =$ 174.6 Ω. Then, the magnitude of R_m^1 ($\cong 26.5$ Ω) is about 15.2 percentages of the magnitude of R_m^A ($\cong 174.6$ Ω). These observations (1)–(4) prove that the magnitude of R_m is sensitive to the vibration amplitude. Furthermore,

the open-circuit method applied to estimate the values of R_m and R_d is more effective than the published methods [1,2], and the impedance of the measuring system influences the estimation of R_d.

7. Conclusions

The waveforms of the transient response are obtained after about 2 ms at the open-circuited time due to the delay of the switch system, and the maximum amplitude of waveforms is obtained at the open-circuited time t_1 or t_3 in Fig. 3(a). Then, the maximum amplitude is about 65 times the voltage of the source at the resonant frequency, and used to quantify the electrical shock. Moreover, the DC time exceeds the AC time; the AC and DC times are used to estimate R_m and R_d, respectively, and the estimated result of R_m^1 is about 15.2 percentages of the magnitude of R_m^A. Thus the resistances in the equivalent circuit are sensitive to the amplitude of vibration, but the inductance and capacitances are not. Furthermore, the impedance of the measuring system influences the DC time and the estimation of R_d. The refined circuit will be applied to accurately estimate the real losses and the motional current.

Appendix A

From Fig. 1(a), the terminal voltage, $V_{oc}(S)$, is derived using the Laplace transformation and the Kirchoff current law, and then expressed by,

$$V_{oc}(S) = L\{v_{oc}(t)\}$$
$$= \frac{b}{S + \alpha_{dc}} + \frac{c(S + \alpha_{ac})}{(S + \alpha_{ac})^2 + \beta^2} + \frac{d(\beta)}{(S + \alpha_{ac})^2 + \beta^2}$$
(A.1)

where

$$\alpha_{dc} = \frac{1}{R_d C_d}, \quad \alpha_{ac} = \frac{R_m}{2L_m} \gg \alpha_{dc},$$

$$\beta = \sqrt{\frac{1}{L_m}\left(\frac{1}{C_m} + \frac{1}{C_d}\right) - \frac{R_m^2}{4L_m^2}},$$

$$b = V_{od} + \frac{(\alpha_{dc}I_0/C_d) + (V_{om}/L_mC_d)}{\alpha_{dc}^2 - 2\alpha_{dc}\alpha_{ac} + (1/L_mC_m)}, \quad c = V_{od} - b$$

and

$$d = \frac{(\alpha_{dc} - \alpha_{ac})\frac{V_{om}}{L_mC_d} + \frac{I_0}{C_d}\left(\alpha_{dc}\alpha_{ac} - \frac{1}{L_mC_m}\right)}{\beta\left(\alpha_{dc}^2 - 2\alpha_{dc}\alpha_{ac} + \frac{1}{L_mC_m}\right)}.$$

Generally,

$$b \cong V_{od} + \frac{C_m}{C_d}(\alpha_{dc}L_mI_0 + V_{om}),$$

$$d \cong \frac{1}{\beta C_d}(C_m(\alpha_{dc} - \alpha_{ac})V_{om} - I_0),$$

$$\beta \cong \sqrt{\frac{1}{L_m}\left(\frac{1}{C_m} + \frac{1}{C_d}\right)}.$$

Furthermore, the voltage, $v_{oc}(t)$, is further calculated by the inverse Laplace transformation, and expressed by,

$$v_{oc}(t) = L^{-1}\{V_{oc}(S)\} \cong be^{-\alpha_{dc}t} + fe^{-\alpha_{ac}t}\cos(\beta t - \varphi)$$
(A.2)

where $f = \sqrt{c^2 + d^2}$ and $\varphi = \arctan\left(\frac{d}{c}\right)$.

References

[1] S. Hirose, New method for measuring mechanical vibration loss and dielectric loss of piezoelectric transducer under high-power excitation, Jpn. J. Appl. Phys. 33 (1994) 2945–2948.
[2] M. Umeda, K. Nakamura, S. Ueha, The measurement of high-power characteristics for a piezoelectric transducer based on the electrical transient response, Jpn. J. Appl. Phys. 37 (1998) 5322–5325.
[3] G.C. Hsieh, C.H. Lin, J.M. Li, Y.C. Hsu, A study of series-resonant DC/AC inverter, IEEE Trans. Power Electron. 11 (1996) 641–652.